SCIENCE CHINA
Information Sciences

• RESEARCH PAPER •

November 2020, Vol. 63 212201:1–212201:16
https://doi.org/10.1007/s11432-019-2664-7

Variable-sampling-period dependent global stabilization of delayed memristive neural networks based on refined switching event-triggered control

Zhilian YAN[1], Xia HUANG[1*] & Jinde CAO[2]

[1]*College of Electrical Engineering and Automation, Shandong University of Science and Technology, Qingdao* 266590*, China;*
[2]*School of Mathematics, Southeast University, Nanjing* 210096*, China*

Received 11 June 2019/Accepted 2 September 2019/Published online 9 October 2020

Abstract This paper studies the stabilization problem of delayed memristive neural networks under event-triggered control. A refined switching event-trigger scheme that switches between variable sampling and continuous event-trigger can be designed by introducing an exponential decay term into the threshold function. Compared with the existing mechanisms, the proposed scheme can enlarge the interval between two successively triggered events and therefore can reduce the amount of triggering times. By constructing a time-dependent and piecewise-defined Lyapunov functional, a less-conservative criterion can be derived to ensure global stability of the closed-loop system. Based on matrix decomposition, equivalent conditions in linear matrix inequalities form of the above stability criterion can be established for the co-design of both the trigger matrix and the feedback gain. A numerical example is provided to demonstrate the effectiveness of the theoretical analysis and the advantages of the refined switching event-trigger scheme.

Keywords event-triggered control, delayed memristive neural networks, global stabilization, time-dependent Lyapunov functional, variable sampling

Citation Yan Z L, Huang X, Cao J D. Variable-sampling-period dependent global stabilization of delayed memristive neural networks based on refined switching event-triggered control. Sci China Inf Sci, 2020, 63(11): 212201, https://doi.org/10.1007/s11432-019-2664-7

1 Introduction

Over the past decade, memristive neural networks (MNNs), whose connection weights are implemented and determined through the use of memristors [1], have received considerable research attention [2–9]. Unlike the traditional neural networks, MNNs have more powerful storage and computing capacities, thus, resulting to their applicability in various application areas such as data storage, secure communication, and image processing [10,11]. It is a well-known fact that the stability of MNNs is the basic precondition for these applications. However, an MNN is naturally a switched system, and the switching law is majorly dependent on the evolution of system states. To be more specific, the MNN with n neurons consists of 2^n subsystems. Such a switching characteristic may lead to undesirable dynamical phenomena such as oscillation, bifurcation, and even chaos. Furthermore, time-delays are inevitable in the hardware implementation of MNNs because of the finite switching speed of amplifiers [12]. They are often one of the primary reasons for the degradation of system performance. Hence, the stabilization issue of delayed memristive neural networks (DMNNs) is extremely significant and many meaningful results have been reported [13–17]. However, it is noteworthy that the control methods involved in the aforementioned

* Corresponding author (email: huangxia_qd@126.com)

literature for stabilization of DMNNs are mostly point-to-point control, except the method proposed in [17]. It should be noted that a prerequisite for point-to-point control is that sensors must send the signals to controllers in a continuous way. It may result in the over-occupation of limited network resources.

Owing to the rapid development of computer network and communication technology in recent years, considerable attention has been paid to networked control systems (NCSs) [18, 19]. NCS is naturally a kind of spatially distributed system in which plants, sensors, actuators, and controllers are linked through a shared digital communication network [20]. NCSs have many great features such as low installation and maintenance costs, flexible system architecture, and increased reliability compared with the conventional control systems. Because of these competitive advantages, NCS has potential applications in various fields including smart grids, aircraft, and mobile sensor networks [21, 22]. However, the digital communication network is usually constrained by the limited bandwidth and energy sources. Therefore, how to design an energy-efficient communication protocol to relieve the over-occupation of communication channels has become the most urgent problem facing NCS. Event-triggered control (ETC), as a perfect candidate, has been proposed as it strikes a balance between network resources and the system performance. An ETC contains an event generator, which is placed between the sensor and the controller. The sampling action can be executed and the new measurement can be sent to update the controller only when the relative change between the current state and the latest measurement exceeds a predefined threshold. By doing so, the network communication burden can be effectively mitigated, meanwhile, a satisfactory closed-loop performance can be maintained.

It is noteworthy that studies on ETC have hitherto received the attention of researchers in different disciplines. As a result, several effective event-trigger mechanisms have been proposed. First, a continuous ETC was proposed to investigate the input-to-state stability of a closed-loop system in [23]. For the continuous ETC, the sensors need to continuously detect the event-trigger conditions to determine whether to transmit the sampled data or not. It can significantly reduce the frequency of data transmission and thus, avoid unnecessary energy consumption. However, in some cases, especially in the presence of measurement noise or external disturbances, continuous ETC can result in the Zeno phenomenon, which makes it inapplicable for many real-world systems [24]. To solve this problem, a periodic ETC, which tries to strike a balance between periodic sampled-data control and continuous ETC, has been proposed for linear systems [25]. In addition, several other event-trigger mechanisms such as threshold-dependent ETC and sampled-based ETC, have been proposed. For more details, interested readers refer to [26–32] and the references cited therein.

Recently, a switching event-triggered control (SETC) was proposed in [33] for linear systems with polytopic-type uncertainties. Compared with the aforementioned ETC, SETC switches between the periodic sampling and continuous event-trigger. It can guarantee a positive minimal interval between any two successively triggered events. Hence, SETC not only can eliminate the Zeno phenomenon but can also significantly reduce the frequency of data transmission. Subsequent studies have confirmed that SETC is effective and technically feasible [34–36]. However, the following issues need to be considered. (1) Generally speaking, a relatively large threshold function in the triggering condition implies a smaller probability that the event will be triggered. Therefore, how to moderately increase the threshold function in SETC to further reduce the triggering times is a question worthy of an in-depth discussion. (2) In engineering, the aperiodic sampling approach is more reasonable and practicable than periodic sampling if intermittent sensor breakdown is considered. Hence, how to refine the existing SETC mechanism is of great theoretical and practical significance.

Inspired by the foregoing discussions, this paper addresses the global stabilization of DMNNs via a refined switching event-triggered control (RSETC). The main contributions of this paper are as follows: (1) A refined SETC, in which periodic sampling is replaced by aperiodic sampling and an exponential function is introduced into the predefined threshold function, is proposed. The refined SETC can further enlarge the interval between two successively triggered events and thus can reduce the triggering times. (2) A time-dependent and piecewise-defined Lyapunov functional is constructed to obtain less conservative criteria for global stabilization of the DMNNs. (3) We also propose a way in which co-design of the trigger matrix and the feedback gain can be fulfilled by solving a set of linear matrix inequalities (LMIs).

Notations. Throughout this paper, $\mathbb{R}$ and $\mathbb{R}^n$ refer to the real space and the n-dimensional Euclidean space, respectively. For a matrix A, $A > 0$ ($A < 0$) implies that A is a symmetric positive definite (respectively, symmetric negative definite) matrix. A^{T} and A^{-1} denote the transpose and the inverse of matrix A, respectively. $\mathscr{S}(A)$ represents the expression $A + A^{\mathrm{T}}$. $\mathrm{diag}\{\cdot, \cdots, \cdot\}$ represents a diagonal matrix. I and 0 denote an identity matrix and zero matrix with appropriate dimensions, respectively. $\mathrm{col}\{\cdot\}$ represents a column vector. In block symmetric matrices, the symbol $*$ is used to represent the elements induced using symmetry. In addition, $C([a, b], \mathbb{R}^n)$ represents a family of continuous functions from $[a, b]$ to $\mathbb{R}^n$, and $C^1([a, b], \mathbb{R}^n)$ denotes a family of continuously differentiable functions from $[a, b]$ to $\mathbb{R}^n$.

2 Problem formulation and preliminaries

Consider the following DMNNs with n-neuron:

$$\dot{x}_i(t) = -d_i x_i(t) + \sum_{j=1}^{n} a_{ij}(x_j(t)) f_j(x_j(t)) + \sum_{j=1}^{n} b_{ij}(x_j(t)) f_j(x_j(t - \tau(t))) + u_i(t), \tag{1}$$

where $x_i(t)$, $i = 1, 2, \ldots, n$, denotes the state of the ith neuron; $d_i > 0$ denotes the self-inhibition of the ith neuron; $\tau(t)$ denotes the time-varying delay of system (1) that satisfies the constraints $0 \leqslant \tau(t) \leqslant \tau$ and $\dot{\tau}(t) \leqslant \mu < 1$; $f_j(\cdot)$ represents the activation function of the jth neuron that satisfies the condition $f_j(0) = 0$; and $u_i(t)$ denotes the control input. The memristive connection weights $a_{ij}(x_j(t))$ and $b_{ij}(x_j(t))$ can be defined as

$$a_{ij}(x_j(t)) = \begin{cases} a'_{ij}, & |x_j(t)| \leqslant T_j, \\ a''_{ij}, & |x_j(t)| > T_j, \end{cases} \quad b_{ij}(x_j(t)) = \begin{cases} b'_{ij}, & |x_j(t)| \leqslant T_j, \\ b''_{ij}, & |x_j(t)| > T_j, \end{cases}$$

where $T_j > 0$ refers to the switching jump, and a'_{ij}, a''_{ij}, b'_{ij}, b''_{ij} are constants satisfying the condition $a'_{ij} \neq a''_{ij}$, $b'_{ij} \neq b''_{ij}$ for $i, j = 1, 2, \ldots, n$. The initial conditions of DMNNs (1) are assumed to be $x_i(t) = \varphi_i(t) \in C([-\tau, 0], \mathbb{R})$.

It is noteworthy that owing to the discontinuity of $a_{ij}(\cdot)$ and $b_{ij}(\cdot)$, DMNNs (1) is fundamentally a system that can be described using a class of differential equations with discontinuous right-hand sides. The solutions of system (1) should be considered in the Filippov's sense. Next, we introduce the definition of Filippov solution.

Definition 1 ([37])**.** Consider the system $\dot{x}(t) = f(t, x)$, $x \in \mathbb{R}^n$, with discontinuous right-hand sides. A set-valued map can be defined as

$$F(t, x) = \bigcap_{\varsigma > 0} \bigcap_{\mu(N) = 0} \overline{\mathrm{co}}[f(t, B(x, \varsigma) \backslash N)],$$

where $\overline{\mathrm{co}}[E]$ represents the closure of the convex hull of set E, $B(x, \varsigma) = \{y : \|y - x\| \leqslant \varsigma, y \in \mathbb{R}^n, \varsigma > 0\}$, and $\mu(N)$ represents the Lebesgue measure of set N. A solution in Filippov's sense for the above system with initial condition $x(0) = x_0$ is an absolutely continuous function $x(t)$, $t \in [0, T)$, which satisfies the condition $x(0) = x_0$ and differential inclusion

$$\dot{x}(t) \in F(t, x)$$

for a.e. $t \in [0, T)$.

Let $a_{ij} = \max\{a'_{ij}, a''_{ij}\}$, $\tilde{a}_{ij} = \min\{a'_{ij}, a''_{ij}\}$, $b_{ij} = \max\{b'_{ij}, b''_{ij}\}$, $\tilde{b}_{ij} = \min\{b'_{ij}, b''_{ij}\}$, $\hat{a}_{ij} = \frac{a_{ij} + \tilde{a}_{ij}}{2}$, $\check{a}_{ij} = \frac{a_{ij} - \tilde{a}_{ij}}{2}$, $\hat{b}_{ij} = \frac{b_{ij} + \tilde{b}_{ij}}{2}$, $\check{b}_{ij} = \frac{b_{ij} - \tilde{b}_{ij}}{2}$. According to differential inclusion theory [38] and Definition 1, it follows that

$$\dot{x}_i(t) \in -d_i x_i(t) + \sum_{j=1}^{n} (\hat{a}_{ij} + \check{a}_{ij} \mathrm{co}\{-1, 1\}) f_j(x_j(t)) + \sum_{j=1}^{n} (\hat{b}_{ij} + \check{b}_{ij} \mathrm{co}\{-1, 1\}) f_j(x_j(t - \tau(t))) + u_i(t),$$

where $\mathrm{co}\{-1,1\}=[-1,1]$. In the light of the measurable selection theorem [38], there exist measurable functions $\Delta_{ij}^1(t)\in\mathrm{co}\{-1,1\}$ and $\Delta_{ij}^2(t)\in\mathrm{co}\{-1,1\}$, such that

$$\dot{x}_i(t)=-d_ix_i(t)+\sum_{j=1}^{n}(\hat{a}_{ij}+\check{a}_{ij}\Delta_{ij}^1(t))f_j(x_j(t))+\sum_{j=1}^{n}(\hat{b}_{ij}+\check{b}_{ij}\Delta_{ij}^2(t))f_j(x_j(t-\tau(t)))+u_i(t). \quad (2)$$

Let $x(t)=[x_1(t),x_2(t),\ldots,x_n(t)]^{\mathrm{T}}$, $D=\mathrm{diag}\{d_1,d_2,\ldots,d_n\}$, $A=[\hat{a}_{ij}]_{n\times n}$, $B=[\hat{b}_{ij}]_{n\times n}$, $f(x(t))=[f_1(x_1(t)),f_2(x_2(t)),\ldots,f_n(x_n(t))]^{\mathrm{T}}$, $\Delta_k(t)=\mathrm{diag}\{\Delta_{11}^k(t),\ldots,\Delta_{1n}^k(t),\ldots,\Delta_{n1}^k(t),\ldots,\Delta_{nn}^k(t)\}$, $A_1=[\sqrt{\check{a}_{11}}\delta_1,\ldots,\sqrt{\check{a}_{1n}}\delta_1,\ldots,\sqrt{\check{a}_{n1}}\delta_n,\ldots,\sqrt{\check{a}_{nn}}\delta_n]_{n\times n^2}$, $A_2^{\mathrm{T}}=[\sqrt{\check{a}_{11}}\delta_1,\ldots,\sqrt{\check{a}_{1n}}\delta_n,\ldots,\sqrt{\check{a}_{n1}}\delta_1,\ldots,\sqrt{\check{a}_{nn}}\delta_n]_{n\times n^2}$, $B_1=[\sqrt{\check{b}_{11}}\delta_1,\ldots,\sqrt{\check{b}_{1n}}\delta_1,\ldots,\sqrt{\check{b}_{n1}}\delta_n,\ldots,\sqrt{\check{b}_{nn}}\delta_n]_{n\times n^2}$, $B_2^{\mathrm{T}}=[\sqrt{\check{b}_{11}}\delta_1,\ldots,\sqrt{\check{b}_{1n}}\delta_n,\ldots,\sqrt{\check{b}_{n1}}\delta_1,\ldots,\sqrt{\check{b}_{nn}}\delta_n]_{n\times n^2}$, $u(t)=[u_1(t),u_2(t),\ldots,u_n(t)]^{\mathrm{T}}$, in which $\delta_i\in\mathbb{R}^n$ represents a column vector with i-element being 1 and the other elements being 0, and $\Delta_k(t)\Delta_k(t)\leqslant I$ for $k=1,2$. Thus, system (2) can be recast as the following compact form:

$$\dot{x}(t)=-Dx(t)+(A+A_1\Delta_1(t)A_2)f(x(t))+(B+B_1\Delta_2(t)B_2)f(x(t-\tau(t)))+u(t). \quad (3)$$

This paper aims to address the stabilization problem of DMNNs (1) within the framework of ETC. An RSETC scheme can be devised to stabilize system (1). First, the event-trigger-based sampling instants are represented as $0=t_0<t_1<\cdots<t_k<\cdots$, $\lim_{k\to\infty}t_k=\infty$. The working principle of the RSETC is as follows. Suppose the measurement $x(t_k)$ is transmitted to the controller at the instant t_k. Subsequently, the sensor waits for h_k seconds. At the instant t_k+h_k, the sensor starts to continuously supervise the event-triggering condition. Once the condition is satisfied, the sensor will send the new measurement $x(t_{k+1})$ to update the controller at the instant t_{k+1}. Then, the event-triggering condition to determine the sampling instants can be defined as

$$t_{k+1}=\min\left\{t\geqslant t_k+h_k \mid (x(t)-x(t_k))^{\mathrm{T}}\Omega(x(t)-x(t_k))>\gamma x^{\mathrm{T}}(t)\Omega x(t)+\alpha\mathrm{e}^{-\beta t}\right\}, \quad (4)$$

where $\Omega\geqslant 0$ refers to the trigger matrix, $\alpha\geqslant 0$, $\beta>0$, and $\gamma\geqslant 0$ are given scalars, and h_k denotes the variable sampling-period that satisfies the condition $h_k\in[\lambda_1,\lambda_2]$, where λ_1 and λ_2 ($\lambda_2\geqslant\lambda_1>0$) are the known lower and upper bounds of h_k, respectively. The controller can be designed on the basis of the above event-triggering mechanism as follows:

$$u(t)=-Fx(t_k), \quad t\in[t_k,t_{k+1}), \quad (5)$$

where F denotes the feedback gain to be determined later. Note that the control inputs are only updated at the sampling instants, and the zero-order holder is used to maintain the continuity of the control signal.

Remark 1. Note that RSETC (4) combines the idea of SETC and a novel threshold function in a comprehensive way. The newly-designed triggering mechanism switches between the variable sampling and continuous event-trigger mechanisms, which can not only prevent the Zeno phenomenon but also lighten the heavy workload of the communication network. Specifically, unlike the existing event-trigger mechanisms [26, 29, 33–35], the predefined threshold function in RSETC (4) consists of two parts. In addition to the common term $\gamma x(t)^{\mathrm{T}}\Omega x(t)$, the other term $\alpha\mathrm{e}^{-\beta t}$ is intentionally introduced into the threshold function. Owing to the incorporation of $\alpha\mathrm{e}^{-\beta t}$, the threshold function in the event-triggering condition can become relatively large, which may postpone the triggering time of the next required data and thus can result in further network resource savings. We demonstrate the advantages of the proposed event-trigger mechanism (4) in Section 4 by comparing it with some existing event-triggering mechanisms.

Remark 2. It is noteworthy that, unlike the periodic sampling in SETC mechanism [33–35], the sampling period h_k in triggering condition (4) lies in the interval $[\lambda_1,\lambda_2]$. Thus, it implies that the break time for sensors is not necessarily constant and may vary between λ_1 and λ_2. Actually, the sampling period cannot remain invariant all the time in practical control systems owing to the undesirable physical environments such as intermittent sensor breakdown that may exist. Therefore, variable sampling is more general and practical. In particular, the RSETC (4) can degenerate into the variable sampling as presented in [39,40] when $\alpha = \gamma = 0$. It can also degenerate into the SETC scheme as reported in [33–35] when $\alpha = 0$ and $h_k = h$.

Under controller (5), system (3) can be expressed as

$$\dot{x}(t) = -Dx(t) + (A + A_1\Delta_1(t)A_2)f(x(t)) + (B + B_1\Delta_2(t)B_2)f(x(t-\tau(t))) - Fx(t_k). \tag{6}$$

Particularly, system (6) with event-trigger mechanism (4) can be treated as a system under variable sampling for $t \in [t_k, t_k + h_k)$, and as a system under continuous event-trigger for $t \in [t_k + h_k, t_{k+1})$. Thus, system (6) can be rewritten as the following two subsystems:

$$\dot{x}(t) = -Dx(t) + (A + A_1\Delta_1(t)A_2)f(x(t)) + (B + B_1\Delta_2(t)B_2)f(x(t-\tau(t))) - Fx(t-\rho(t)),\ t \in [t_k, t_k + h_k), \tag{7}$$

$$\dot{x}(t) = -Dx(t) + (A + A_1\Delta_1(t)A_2)f(x(t)) + (B + B_1\Delta_2(t)B_2)f(x(t-\tau(t))) - Fx(t_k),\ t \in [t_k + h_k, t_{k+1}), \tag{8}$$

where $\rho(t)$ is defined as $\rho(t) \triangleq t - t_k$, for $t \in [t_k, t_k + h_k)$. In this paper, $\rho(t)$ is regarded as the input delay. Obviously, $\rho(t) < h_k$.

In this paper, the following assumption and lemmas are introduced.

Assumption 1. The activation function $f_i(\cdot)$ satisfies the following condition:

$$m_i^- \leqslant \frac{f_i(x) - f_i(y)}{x - y} \leqslant m_i^+, \quad \text{for } x, y \in \mathbb{R},\ x \neq y,\ i = 1, 2, \ldots, n,$$

where m_i^- and m_i^+ denote the given constants.

Lemma 1 ([41]). For a given matrix $M > 0$ and a continuously differentiable function $e(s) \in C^1([a,b], \mathbb{R}^n)$, the following inequality holds:

$$-\int_a^b \dot{e}^{\mathrm{T}}(s)M\dot{e}(s)\mathrm{d}s \leqslant -\frac{1}{b-a}v^{\mathrm{T}} \begin{bmatrix} 4M & 2M & -6M \\ * & 4M & -6M \\ * & * & 12M \end{bmatrix} v$$

in which $v = \mathrm{col}\{e(b), e(a), \frac{1}{b-a}\int_a^b e(s)\mathrm{d}s\}$.

Lemma 2 ([42]). For a real scalar $\varepsilon > 0$ and real matrices Λ, U_i, V_i and W_i $(i = 1, \ldots, n)$, if the following condition:

$$\begin{bmatrix} \Lambda & U_1 + \varepsilon V_1 \ \cdots \ U_n + \varepsilon Vn \\ * & \mathrm{diag}\{\, -\varepsilon\mathscr{S}(W_1),\ \ldots,\ -\varepsilon\mathscr{S}(W_n)\,\} \end{bmatrix} < 0$$

holds, then

$$\Lambda + \sum_{i=1}^{n} \mathscr{S}\left(U_i W_i^{-1} V_i^{\mathrm{T}}\right) < 0.$$

3 Main results

In this section, we first derive some sufficient conditions to guarantee the globally asymptotical stability of the closed-loop system (6). Subsequently, the design method for the feedback gain is proposed based on the sufficient conditions obtained to ensure the global stabilization of the DMNNs (1).

Theorem 1. For given scalars $\alpha \geqslant 0$, $\beta > 0$, $\gamma \geqslant 0$, $\delta > 0$, $\lambda_2 \geqslant \lambda_1 > 0$ and feedback gain F, the closed-loop system (6) is globally asymptotically stable, if there exist matrices $P > 0$, $Q > 0$, $R > 0$, $S > 0$, $U > 0$, $\Omega \geqslant 0$, diagonal matrices $N_1 > 0$, $N_2 > 0$, $Z_1 > 0$, $Z_2 > 0$, $Z_3 > 0$, $Z_4 > 0$, and arbitrary matrices Y_1, Y_2, X, X_1, $\forall h_k \in [\lambda_1, \lambda_2]$, satisfying the following constraints:

$$\Pi_1(h_k) = \begin{bmatrix} P + h_k\dfrac{\mathscr{S}(X)}{2} & h_k(-X + X_1) \\ * & h_k\left(-\mathscr{S}(X_1) + \dfrac{\mathscr{S}(X)}{2}\right) \end{bmatrix} > 0, \tag{9}$$

$$\Pi_2(h_k)=\begin{bmatrix}\Sigma(h_k) & \xi_1 & \xi_2 & \xi_3 & \xi_4\\ * & -Z_1 & 0 & 0 & 0\\ * & * & -Z_2 & 0 & 0\\ * & * & * & -Z_3 & 0\\ * & * & * & * & -Z_4\end{bmatrix}<0, \tag{10}$$

$$\Pi_3(h_k)=\begin{bmatrix}\Theta(h_k) & \xi_1 & \xi_2 & \xi_3 & \xi_4\\ * & -Z_1 & 0 & 0 & 0\\ * & * & -Z_2 & 0 & 0\\ * & * & * & -Z_3 & 0\\ * & * & * & * & -Z_4\end{bmatrix}<0, \tag{11}$$

$$\Pi_4=\begin{bmatrix}\Gamma & \eta_1 & \eta_2 & \eta_3 & \eta_4\\ * & -Z_1 & 0 & 0 & 0\\ * & * & -Z_2 & 0 & 0\\ * & * & * & -Z_3 & 0\\ * & * & * & * & -Z_4\end{bmatrix}<0, \tag{12}$$

where $\Sigma(h_k)=[\Sigma_{ij}]_{9n\times 9n}$, $\Theta(h_k)=[\Theta_{ij}]_{9n\times 9n}$, $\Gamma=[\Gamma_{ij}]_{8n\times 8n}$ are symmetric matrices, and $\Sigma_{11}=2\delta P+Q-\frac{4R}{\tau}\mathrm{e}^{-2\delta\tau}+h_kS+\frac{\delta\lambda_2 h_k}{2}S-\frac{4U}{\lambda_2}\mathrm{e}^{-2\delta\lambda_2}+\frac{2\delta h_k-1}{2}\mathscr{S}(X)-Y_1^{\mathrm{T}}D-DY_1-M_1N_1$, $\Sigma_{12}=P+\frac{h_k}{2}\mathscr{S}(X)+\frac{\lambda_2 h_k}{4}S-Y_1^{\mathrm{T}}-DY_2$, $\Sigma_{14}=-\frac{2U}{\lambda_2}\mathrm{e}^{-2\delta\lambda_2}-Y_1^{\mathrm{T}}F+(2\delta h_k-1)(-X+X_1)$, $\Sigma_{15}=\Theta_{15}=\Gamma_{15}=-\frac{2R}{\tau}\mathrm{e}^{-2\delta\tau}$, $\Sigma_{16}=\Theta_{16}=\Gamma_{16}=\frac{6R}{\tau}\mathrm{e}^{-2\delta\tau}$, $\Sigma_{17}=\Theta_{17}=\frac{6U}{\lambda_2}\mathrm{e}^{-2\delta\lambda_2}$, $\Sigma_{18}=\Theta_{18}=\Gamma_{17}=Y_1^{\mathrm{T}}A+M_2N_1$, $\Sigma_{19}=\Theta_{19}=\Gamma_{18}=Y_1^{\mathrm{T}}B$, $\Sigma_{22}=\tau R+h_kU-Y_2^{\mathrm{T}}-Y_2$, $\Sigma_{24}=h_k(-X+X_1)-Y_2^{\mathrm{T}}F$, $\Sigma_{28}=\Theta_{28}=\Gamma_{27}=Y_2^{\mathrm{T}}A$, $\Sigma_{29}=\Theta_{29}=\Gamma_{28}=Y_2^{\mathrm{T}}B$, $\Sigma_{33}=\Theta_{33}=\Gamma_{33}=-(1-\mu)\mathrm{e}^{-2\delta\tau}Q-M_1N_2$, $\Sigma_{39}=\Theta_{39}=\Gamma_{38}=M_2N_2$, $\Sigma_{44}=-\frac{4U}{\lambda_2}\mathrm{e}^{-2\delta\lambda_2}+(2\delta h_k-1)(\frac{\mathscr{S}(X)}{2}-\mathscr{S}(X_1))$, $\Sigma_{47}=\Theta_{47}=\frac{6U}{\lambda_2}\mathrm{e}^{-2\delta\lambda_2}$, $\Sigma_{55}=\Theta_{55}=\Gamma_{55}=-\frac{4R}{\tau}\mathrm{e}^{-2\delta\tau}$, $\Sigma_{56}=\Theta_{56}=\Gamma_{56}=\frac{6R}{\tau}\mathrm{e}^{-2\delta\tau}$, $\Sigma_{66}=\Theta_{66}=\Gamma_{66}=-\frac{12R}{\tau}\mathrm{e}^{-2\delta\tau}$, $\Sigma_{77}=\Theta_{77}=-\frac{12U}{\lambda_2}\mathrm{e}^{-2\delta\lambda_2}$, $\Sigma_{88}=\Theta_{88}=\Gamma_{77}=A_2^{\mathrm{T}}(Z_1+Z_3)A_2-N_1$, $\Sigma_{99}=\Theta_{99}=\Gamma_{88}=B_2^{\mathrm{T}}(Z_2+Z_4)B_2-N_2$, $\Theta_{11}=\Sigma_{11}-2h_kS-\delta h_k\mathscr{S}(X)$, $\Theta_{12}=\Sigma_{12}-\frac{h_k}{2}\mathscr{S}(X)$, $\Theta_{14}=\Sigma_{14}-2\delta h_k(-X+X_1)$, $\Theta_{22}=\Gamma_{22}=\Sigma_{22}-h_kU$, $\Theta_{24}=\Gamma_{24}=-Y_2^{\mathrm{T}}F$, $\Theta_{44}=\Sigma_{44}+2\delta h_k(\mathscr{S}(X_1)-\frac{\mathscr{S}(X)}{2})$, $\Gamma_{11}=2\delta P+Q-\frac{4R}{\tau}\mathrm{e}^{-2\delta\tau}+\gamma\Omega-\Omega-Y_1^{\mathrm{T}}D-DY_1-M_1N_1$, $\Gamma_{12}=P-Y_1^{\mathrm{T}}-DY_2$, $\Gamma_{14}=\Omega-Y_1^{\mathrm{T}}F$, $\Gamma_{44}=-\Omega$, other blocks represent zero matrices and $\xi_1=\mathrm{col}\{Y_1^{\mathrm{T}}A_1,0_{8n\times n}\}$, $\xi_2=\mathrm{col}\{Y_1^{\mathrm{T}}B_1,0_{8n\times n}\}$, $\xi_3=\mathrm{col}\{0_{n\times n},Y_2^{\mathrm{T}}A_1,0_{7n\times n}\}$, $\xi_4=\mathrm{col}\{0_{n\times n},Y_2^{\mathrm{T}}B_1,0_{7n\times n}\}$, $\eta_1=\mathrm{col}\{Y_1^{\mathrm{T}}A_1,0_{7n\times n}\}$, $\eta_2=\mathrm{col}\{Y_1^{\mathrm{T}}B_1,0_{7n\times n}\}$, $\eta_3=\mathrm{col}\{0_{n\times n},Y_2^{\mathrm{T}}A_1,0_{6n\times n}\}$, $\eta_4=\mathrm{col}\{0_{n\times n},Y_2^{\mathrm{T}}B_1,0_{6n\times n}\}$.

Proof. Choose a time-dependent and piecewise-defined Lyapunov functional defined as follows:

$$V(t)=\begin{cases}\bar{V}(t)=\sum_{i=1}^{6}V_i(t), & t\in[t_k,t_k+h_k),\\ \widetilde{V}(t)=\sum_{i=1}^{3}V_i(t), & t\in[t_k+h_k,t_{k+1}),\end{cases}$$

where

$$\begin{aligned}V_1(t)&=x^{\mathrm{T}}(t)Px(t),\\ V_2(t)&=\int_{t-\tau(t)}^{t}\mathrm{e}^{2\delta(s-t)}x^{\mathrm{T}}(s)Qx(s)\mathrm{d}s,\\ V_3(t)&=\int_{t-\tau}^{t}\int_{\theta}^{t}\mathrm{e}^{2\delta(s-t)}\dot{x}^{\mathrm{T}}(s)R\dot{x}(s)\mathrm{d}s\mathrm{d}\theta,\\ V_4(t)&=\rho_1(t)\rho(t)x^{\mathrm{T}}(t)Sx(t),\\ V_5(t)&=\rho_1(t)\int_{t-\rho(t)}^{t}\mathrm{e}^{2\delta(s-t)}\dot{x}^{\mathrm{T}}(s)U\dot{x}(s)\mathrm{d}s,\end{aligned}$$

$$V_6(t) = \rho_1(t)\begin{bmatrix} x(t) \\ x(t-\rho(t)) \end{bmatrix}^{\mathrm{T}} \begin{bmatrix} \frac{\mathscr{S}(X)}{2} & -X+X_1 \\ * & -\mathscr{S}(X_1)+\frac{\mathscr{S}(X)}{2} \end{bmatrix} \begin{bmatrix} x(t) \\ x(t-\rho(t)) \end{bmatrix},$$

and $\rho_1(t) = t_k + h_k - t$.

First, the inequality (9) can guarantee that $V_1(t) + V_6(t)$ is positive definite as

$$\begin{aligned} V_1(t)+V_6(t) &= \omega^{\mathrm{T}}(t)\begin{bmatrix} P+\rho_1(t)\frac{\mathscr{S}(X)}{2} & \rho_1(t)(-X+X_1) \\ * & \rho_1(t)\left(-\mathscr{S}(X_1)+\frac{\mathscr{S}(X)}{2}\right) \end{bmatrix}\omega(t), \\ &= \omega^{\mathrm{T}}(t)\left(\frac{h_k-\rho_1(t)}{h_k}\begin{bmatrix} P & 0 \\ 0 & 0 \end{bmatrix} + \frac{\rho_1(t)}{h_k}\begin{bmatrix} P+h_k\frac{\mathscr{S}(X)}{2} & h_k(-X+X_1) \\ * & h_k\left(-\mathscr{S}(X_1)+\frac{\mathscr{S}(X)}{2}\right) \end{bmatrix}\right)\omega(t) \\ &= \frac{h_k-\rho_1(t)}{h_k}\omega^{\mathrm{T}}(t)\begin{bmatrix} P & 0 \\ 0 & 0 \end{bmatrix}\omega(t)+\frac{\rho_1(t)}{h_k}\omega^{\mathrm{T}}(t)\begin{bmatrix} P+h_k\frac{\mathscr{S}(X)}{2} & h_k(-X+X_1) \\ * & h_k\left(-\mathscr{S}(X_1)+\frac{\mathscr{S}(X)}{2}\right) \end{bmatrix}\omega(t), \end{aligned}$$

where $\omega(t) = \mathrm{col}\{x(t), x(t-\rho(t))\}$. Obviously, $V_i(t)$, $i = 2, \ldots, 5$ are positive definite. Thus, both $\bar{V}(t)$ and $\widetilde{V}(t)$ are positive definite.

By evaluating the derivative of $V_i(t)$, $i = 1, 2, \ldots, 6$, along the trajectories of the system (6), we obtain

$$\begin{aligned} \dot{V}_1(t) &= 2x^{\mathrm{T}}(t)P\dot{x}(t), \\ \dot{V}_2(t) &= -2\delta V_2(t) + x^{\mathrm{T}}(t)Qx(t) - (1-\dot{\tau}(t))\mathrm{e}^{-2\delta\tau(t)}x^{\mathrm{T}}(t-\tau(t))Qx(t-\tau(t)) \\ &\leqslant -2\delta V_2(t) + x^{\mathrm{T}}(t)Qx(t) - (1-\mu)\mathrm{e}^{-2\delta\tau}x^{\mathrm{T}}(t-\tau(t))Qx(t-\tau(t)), \\ \dot{V}_3(t) &= -2\delta V_3(t) + \tau\dot{x}^{\mathrm{T}}(t)R\dot{x}(t) - \int_{t-\tau}^{t}\mathrm{e}^{2\delta(s-t)}\dot{x}^{\mathrm{T}}(s)R\dot{x}(s)\mathrm{d}s \\ &\leqslant -2\delta V_3(t) + \tau\dot{x}^{\mathrm{T}}(t)R\dot{x}(t) - \mathrm{e}^{-2\delta\tau}\int_{t-\tau}^{t}\dot{x}^{\mathrm{T}}(s)R\dot{x}(s)\mathrm{d}s, \\ \dot{V}_4(t) &= (\rho_1(t)-\rho(t))x^{\mathrm{T}}(t)Sx(t) + 2\rho_1(t)\rho(t)x^{\mathrm{T}}(t)S\dot{x}(t), \\ \dot{V}_5(t) &= -2\delta V_5(t) + \rho_1(t)\dot{x}^{\mathrm{T}}(t)U\dot{x}(t) - \int_{t-\rho(t)}^{t}\mathrm{e}^{2\delta(s-t)}\dot{x}^{\mathrm{T}}(s)U\dot{x}(s)\mathrm{d}s \\ &\leqslant -2\delta V_5(t) + \rho_1(t)\dot{x}^{\mathrm{T}}(t)U\dot{x}(t) - \mathrm{e}^{-2\delta\lambda_2}\int_{t-\rho(t)}^{t}\dot{x}^{\mathrm{T}}(s)U\dot{x}(s)\mathrm{d}s, \\ \dot{V}_6(t) &= -\begin{bmatrix} x(t) \\ x(t-\rho(t)) \end{bmatrix}^{\mathrm{T}} \begin{bmatrix} \frac{\mathscr{S}(X)}{2} & -X+X_1 \\ * & -\mathscr{S}(X_1)+\frac{\mathscr{S}(X)}{2} \end{bmatrix} \begin{bmatrix} x(t) \\ x(t-\rho(t)) \end{bmatrix} \\ &\quad +\rho_1(t)\left[\dot{x}^{\mathrm{T}}(t)(\mathscr{S}(X))x(t) + 2\dot{x}^{\mathrm{T}}(t)(-X+X_1)x(t-\rho(t))\right]. \end{aligned}$$

Based on Lemma 1, we obtain

$$\dot{V}_3(t) \leqslant -2\delta V_3(t) + \tau\dot{x}^{\mathrm{T}}(t)R\dot{x}(t) - \frac{1}{\tau}\mathrm{e}^{-2\delta\tau}\begin{bmatrix} x(t) \\ x(t-\tau) \\ v_1(t) \end{bmatrix}^{\mathrm{T}}\begin{bmatrix} 4R & 2R & -6R \\ * & 4R & -6R \\ * & * & 12R \end{bmatrix}\begin{bmatrix} x(t) \\ x(t-\tau) \\ v_1(t) \end{bmatrix}, \quad (13)$$

$$\dot{V}_5(t) \leqslant -2\delta V_5(t) + \rho_1(t)\dot{x}^{\mathrm{T}}(t)U\dot{x}(t) - \frac{1}{\lambda_2}\mathrm{e}^{-2\delta\lambda_2}\begin{bmatrix} x(t) \\ x(t-\rho(t)) \\ v_2(t) \end{bmatrix}^{\mathrm{T}}\begin{bmatrix} 4U & 2U & -6U \\ * & 4U & -6U \\ * & * & 12U \end{bmatrix}\begin{bmatrix} x(t) \\ x(t-\rho(t)) \\ v_2(t) \end{bmatrix}, \quad (14)$$

where $v_1(t)=\frac{1}{\tau}\int_{t-\tau}^{t}x(s)\mathrm{d}s$, and $v_2(t)=\frac{1}{\rho(t)}\int_{t-\rho(t)}^{t}x(s)\mathrm{d}s$.

With Assumption 1, for diagonal matrices $N_1>0$, $N_2>0$, we obtain

$$\begin{bmatrix} x(t) \\ f(x(t)) \end{bmatrix}^{\mathrm{T}} \begin{bmatrix} -M_1N_1 & M_2N_1 \\ M_2N_1 & -N_1 \end{bmatrix} \begin{bmatrix} x(t) \\ f(x(t)) \end{bmatrix} \geqslant 0, \tag{15}$$

$$\begin{bmatrix} x(t-\tau(t)) \\ f(x(t-\tau(t))) \end{bmatrix}^{\mathrm{T}} \begin{bmatrix} -M_1N_2 & M_2N_2 \\ M_2N_2 & -N_2 \end{bmatrix} \begin{bmatrix} x(t-\tau(t)) \\ f(x(t-\tau(t))) \end{bmatrix} \geqslant 0, \tag{16}$$

where $M_1=\mathrm{diag}\{m_1^-m_1^+, m_2^-m_2^+,\ldots,m_n^-m_n^+\}$, and $M_2=\mathrm{diag}\{\frac{(m_1^-+m_1^+)}{2},\frac{(m_2^-+m_2^+)}{2},\ldots,\frac{(m_n^-+m_n^+)}{2}\}$.

In addition, the following facts are needed to derive the main results:

$$\rho_1(t)\rho(t)\leqslant\frac{(\rho_1(t)+\rho(t))^2}{4}\leqslant\frac{\lambda_2(\rho_1(t)+\rho(t))}{4}.$$

The following proof is divided into two parts according to the segmented intervals: $[t_k,t_k+h_k)$ and $[t_k+h_k,t_{k+1})$.

Case 1. When $t\in[t_k,t_k+h_k)$, for system (7), the Lyapunov functional $\bar{V}(t)=\sum_{i=1}^{6}V_i(t)$ can be employed. In addition, for free-weighting matrices Y_1 and Y_2 with appropriate dimensions, we obtain

$$0=2\left[x^{\mathrm{T}}(t)Y_1^{\mathrm{T}}+\dot{x}^{\mathrm{T}}(t)Y_2^{\mathrm{T}}\right]\left[-\dot{x}(t)-Dx(t)+A(t)f(x(t))+B(t)f(x(t-\tau(t)))-Fx(t-\rho(t))\right], \tag{17}$$

where $A(t)=A+A_1\Delta_1(t)A_2$, and $B(t)=B+B_1\Delta_2(t)B_2$.

Also, for diagonal matrices $Z_1>0$, $Z_2>0$, $Z_3>0$, $Z_4>0$ with appropriate dimensions, we obtain

$$\begin{aligned}
&2x^{\mathrm{T}}(t)Y_1^{\mathrm{T}}A_1\Delta_1(t)A_2f(x(t))\leqslant x^{\mathrm{T}}(t)Y_1^{\mathrm{T}}A_1\Delta_1(t)Z_1^{-1}\Delta_1(t)A_1^{\mathrm{T}}Y_1x(t)+f^{\mathrm{T}}(x(t))A_2^{\mathrm{T}}Z_1A_2f(x(t)),\\
&2x^{\mathrm{T}}(t)Y_1^{\mathrm{T}}B_1\Delta_2(t)B_2f(x(t-\tau(t)))\leqslant x^{\mathrm{T}}(t)Y_1^{\mathrm{T}}B_1\Delta_2(t)Z_2^{-1}\Delta_2(t)B_1^{\mathrm{T}}Y_1x(t)\\
&\qquad+f^{\mathrm{T}}(x(t-\tau(t)))B_2^{\mathrm{T}}Z_2B_2f(x(t-\tau(t))),\\
&2\dot{x}^{\mathrm{T}}(t)Y_2^{\mathrm{T}}A_1\Delta_1(t)A_2f(x(t))\leqslant \dot{x}^{\mathrm{T}}(t)Y_2^{\mathrm{T}}A_1\Delta_1(t)Z_3^{-1}\Delta_1(t)A_1^{\mathrm{T}}Y_2\dot{x}(t)+f^{\mathrm{T}}(x(t))A_2^{\mathrm{T}}Z_3A_2f(x(t)),\\
&2\dot{x}^{\mathrm{T}}(t)Y_2^{\mathrm{T}}B_1\Delta_2(t)B_2f(x(t-\tau(t)))\leqslant \dot{x}^{\mathrm{T}}(t)Y_2^{\mathrm{T}}B_1\Delta_2(t)Z_4^{-1}\Delta_2(t)B_1^{\mathrm{T}}Y_2\dot{x}(t)\\
&\qquad+f^{\mathrm{T}}(x(t-\tau(t)))B_2^{\mathrm{T}}Z_4B_2f(x(t-\tau(t))).
\end{aligned}$$

It is noteworthy that $\Delta_k(t)\Delta_k(t)\leqslant I$ $(k=1,2)$. Thus, we can obtain the following expressions:

$$\begin{aligned}
&2\left[x^{\mathrm{T}}(t)Y_1^{\mathrm{T}}+\dot{x}^{\mathrm{T}}(t)Y_2^{\mathrm{T}}\right]\left[-\dot{x}(t)-Dx(t)+A(t)f(x(t))+B(t)f(x(t-\tau(t)))-Fx(t-\rho(t))\right]\\
&\leqslant 2\left[x^{\mathrm{T}}(t)Y_1^{\mathrm{T}}+\dot{x}^{\mathrm{T}}(t)Y_2^{\mathrm{T}}\right]\left[-\dot{x}(t)-Dx(t)+Af(x(t))+Bf(x(t-\tau(t)))-Fx(t-\rho(t))\right]\\
&\quad+x^{\mathrm{T}}(t)Y_1^{\mathrm{T}}\left[A_1Z_1^{-1}A_1^{\mathrm{T}}+B_1Z_2^{-1}B_1^{\mathrm{T}}\right]Y_1x(t)+\dot{x}^{\mathrm{T}}(t)Y_2^{\mathrm{T}}\left[A_1Z_3^{-1}A_1^{\mathrm{T}}+B_1Z_4^{-1}B_1^{\mathrm{T}}\right]Y_2\dot{x}(t)\\
&\quad+f^{\mathrm{T}}(x(t))A_2^{\mathrm{T}}(Z_1+Z_3)A_2f(x(t))+f^{\mathrm{T}}(x(t-\tau(t)))B_2^{\mathrm{T}}(Z_2+Z_4)B_2f(x(t-\tau(t))).
\end{aligned}\tag{18}$$

According to the inequalities (13)–(18), we can conclude that

$$\dot{\bar{V}}(t)+2\delta\bar{V}(t)\leqslant\xi^{\mathrm{T}}(t)\left[\frac{\rho_1(t)}{h_k}(\Sigma(h_k)+\Xi)+\frac{\rho(t)}{h_k}(\Theta(h_k)+\Xi)\right]\xi(t),$$

where $\xi(t)=\mathrm{col}\{x(t),\dot{x}(t),x(t-\tau(t)),x(t-\rho(t)),x(t-\tau),v_1(t),v_2(t),f(x(t)),f(x(t-\tau(t)))\}$, and $\Xi=\xi_1Z_1^{-1}\xi_1^{\mathrm{T}}+\xi_2Z_2^{-1}\xi_2^{\mathrm{T}}+\xi_3Z_3^{-1}\xi_3^{\mathrm{T}}+\xi_4Z_4^{-1}\xi_4^{\mathrm{T}}$. On the basis of Schur complement [43], $\Sigma(h_k)+\Xi<0$ and $\Theta(h_k)+\Xi<0$ are equivalent to (10) and (11), respectively. Hence, we can conclude that

$$\dot{\bar{V}}(t)+2\delta\bar{V}(t)\leqslant 0,\quad t\in[t_k,t_k+h_k). \tag{19}$$

Case 2. When $t\in[t_k+h_k,t_{k+1})$, for system (8), the Lyapunov functional $\widetilde{V}(t)=\sum_{i=1}^{3}V_i(t)$ can be adopted. Thus, in accordance with (17), we have

$$0=2\left[x^{\mathrm{T}}(t)Y_1^{\mathrm{T}}+\dot{x}^{\mathrm{T}}(t)Y_2^{\mathrm{T}}\right]\left[-\dot{x}(t)-Dx(t)+A(t)f(x(t))+B(t)f(x(t-\tau(t)))-Fx(t_k)\right].$$

A comprehensive analysis of the event-triggering condition (4) and (13)–(18) leads to

$$\dot{\widetilde{V}}(t) + 2\delta\widetilde{V}(t) \leqslant \eta^{\mathrm{T}}(t)(\Gamma + \Gamma_0)\eta(t) + \alpha\mathrm{e}^{-\beta t},$$

where $\eta(t) = \mathrm{col}\{x(t), \dot{x}(t), x(t-\tau(t)), x(t_k), x(t-\tau), v_1(t), f(x(t)), f(x(t-\tau(t)))\}$ and $\Gamma_0 = \eta_1 Z_1^{-1}\eta_1^{\mathrm{T}} + \eta_2 Z_2^{-1}\eta_2^{\mathrm{T}} + \eta_3 Z_3^{-1}\eta_3^{\mathrm{T}} + \eta_4 Z_4^{-1}\eta_4^{\mathrm{T}}$. In the light of Schur complement, $\Gamma + \Gamma_0 < 0$ is equivalent to (12), which shows that

$$\dot{\widetilde{V}}(t) + 2\delta\widetilde{V}(t) \leqslant \alpha\mathrm{e}^{-\beta t}, \quad t \in [t_k + h_k, t_{k+1}). \tag{20}$$

From the definition of $V(t)$, it is clear that

$$V_4(t_k) = V_5(t_k) = V_6(t_k) = 0, \qquad \lim_{t\to(t_k+h_k)^-} V_4(t) = \lim_{t\to(t_k+h_k)^-} V_5(t) = \lim_{t\to(t_k+h_k)^-} V_6(t) = 0.$$

Thus, we have

$$\lim_{t\to t_k} V(t) = V(t_k), \qquad \lim_{t\to t_k+h_k} V(t) = V(t_k+h_k).$$

This implies that $V(t)$ is continuous at t_k and $t_k + h_k$. Thus, the piecewise-defined Lyapunov functional $V(t)$ is continuous on $[0, +\infty)$. For $t \in [t_k + h_k, t_{k+1})$, integrating (20) with respect to t yields

$$\begin{aligned}
V(t) &\leqslant V(t_k + h_k)\mathrm{e}^{-2\delta(t-t_k-h_k)} + \int_{t_k+h_k}^{t} \mathrm{e}^{-2\delta(t-s)}\alpha\mathrm{e}^{-\beta s}\mathrm{d}s \\
&\leqslant V(t_k)\mathrm{e}^{-2\delta(t-t_k)} + \int_{t_k+h_k}^{t} \mathrm{e}^{-2\delta(t-s)}\alpha\mathrm{e}^{-\beta s}\mathrm{d}s \\
&\leqslant V(t_k)\mathrm{e}^{-2\delta(t-t_k)} + \int_{t_k}^{t} \mathrm{e}^{-2\delta(t-s)}\alpha\mathrm{e}^{-\beta s}\mathrm{d}s \\
&\leqslant V(t_{k-1} + h_{k-1})\mathrm{e}^{-2\delta(t-t_{k-1}-h_{k-1})} + \int_{t_{k-1}+h_{k-1}}^{t} \mathrm{e}^{-2\delta(t-s)}\alpha\mathrm{e}^{-\beta s}\mathrm{d}s \\
&\leqslant (V(t_{k-1})\mathrm{e}^{-2\delta h_{k-1}})\mathrm{e}^{-2\delta(t-t_{k-1}-h_{k-1})} + \int_{t_{k-1}+h_{k-1}}^{t} \mathrm{e}^{-2\delta(t-s)}\alpha\mathrm{e}^{-\beta s}\mathrm{d}s \\
&\leqslant V(t_{k-1})\mathrm{e}^{-2\delta(t-t_{k-1})} + \int_{t_{k-1}}^{t} \mathrm{e}^{-2\delta(t-s)}\alpha\mathrm{e}^{-\beta s}\mathrm{d}s \\
&\leqslant \cdots \leqslant V(0)\mathrm{e}^{-2\delta t} + \int_{0}^{t} \mathrm{e}^{-2\delta(t-s)}\alpha\mathrm{e}^{-\beta s}\mathrm{d}s.
\end{aligned}$$

For $t \in [t_k, t_k + h_k)$, repeating the same procedure for (19), we can arrive at the same conclusion. In summary, $V(t)$ can be estimated as

$$V(t) \leqslant \begin{cases} \left(V(0) - \dfrac{\alpha}{2\delta-\beta}\right)\mathrm{e}^{-2\delta t} + \dfrac{\alpha}{2\delta-\beta}\mathrm{e}^{-\beta t}, & \text{if } \beta \neq 2\delta, \\ (V(0) + \alpha t)\mathrm{e}^{-2\delta t}, & \text{if } \beta = 2\delta. \end{cases}$$

When $t \to +\infty$, it is easy to discover that $\mathrm{e}^{-2\delta t} \to 0$, $\mathrm{e}^{-\beta t} \to 0$, and $t\mathrm{e}^{-2\delta t} \to 0$. Hence, the closed-loop system (6) is globally asymptotically stable. Thus, the proof is completed.

Remark 3. It is noteworthy that closed-loop system (6) is actually a time-dependent switched system owing to the introduction of RSETC to the controlled system (1). Thus, how to construct an appropriate Lyapunov functional to analyze the stability of system (6), is a tricky problem. Motivated by [33–35], a time-dependent and piecewise-defined Lyapunov functional $V(t)$ is constructed. To be specific, for the variable sampling interval $[t_k, t_k+h_k)$, the time-dependent Lyapunov functional $\bar{V}(t)$ is employed, and for the continuous event-triggering interval $[t_k + h_k, t_{k+1})$, the time-independent Lyapunov functional $\widetilde{V}(t)$ is adopted. Obviously, the difference between $\bar{V}(t)$ and $\widetilde{V}(t)$ lies on $V_4(t)$, $V_5(t)$, and $V_6(t)$. These three Lyapunov functionals contain the available information of the system states at the points t_k and $t_k + h_k$, which can help to reduce the conservativeness of the obtained stability results. Further, the requirement

$\dot{\widetilde{V}}(t) + 2\delta\widetilde{V}(t) \leqslant 0$ is relaxed to $\dot{\widetilde{V}}(t) + 2\delta\widetilde{V}(t) \leqslant \alpha e^{-\beta t}$ on the interval $[t_k + h_k, t_{k+1})$. This implies that the conservativeness of the obtained results can be further reduced. In addition, it is obvious that the continuity of $V(t)$ at t_k and $t_k + h_k$ plays an important role in the proof of Theorem 1, which guarantees the globally asymptotical stability of system (6) on $[0, +\infty)$.

Owing to the existence of a variable parameter h_k, it is hard to verify the conditions under which Theorem 1 holds. To solve this issue, the following equivalent condition of Theorem 1 is proposed.

Theorem 2. For given scalars $\alpha \geqslant 0$, $\beta > 0$, $\gamma \geqslant 0$, $\delta > 0$, $\lambda_2 \geqslant \lambda_1 > 0$ and feedback gain F, system (6) is globally asymptotically stable, if there exist matrices $P > 0$, $Q > 0$, $R > 0$, $S > 0$, $U > 0$, $\Omega \geqslant 0$, diagonal matrices $N_1 > 0$, $N_2 > 0$, $Z_1 > 0$, $Z_2 > 0$, $Z_3 > 0$, $Z_4 > 0$, and arbitrary matrices Y_1, Y_2, X, X_1, such that for $\tilde{h}_k \in \{\lambda_1, \lambda_2\}$,

$$\Pi_1(\tilde{h}_k) > 0, \quad \Pi_i(\tilde{h}_k) < 0, \text{ and } \Pi_4 < 0 \tag{21}$$

hold, where $\Pi_1(\cdot)$, $\Pi_i(\cdot)$, and Π_4 have the same definition as those in Theorem 1, for $i = 2, 3$.

Proof. Obviously, Theorem 2 can be deduced from Theorem 1, so it is only necessary to prove that Theorem 1 is true if Theorem 2 holds. Because $h_k \in [\lambda_1, \lambda_2]$, it yields $h_k = \theta\lambda_1 + (1-\theta)\lambda_2$, $0 \leqslant \theta \leqslant 1$. From the perspective of Theorem 2, it is clear that $\Pi_1(\lambda_1) > 0$ and $\Pi_1(\lambda_2) > 0$. Owing to the fact that $0 \leqslant \theta \leqslant 1$, it is easy to observe that

$$\begin{aligned}
\Pi_1(h_k) &= \Pi_1(0) + h_k \begin{bmatrix} \dfrac{\mathscr{S}(X)}{2} & -X + X_1 \\ * & -\mathscr{S}(X_1) + \dfrac{\mathscr{S}(X)}{2} \end{bmatrix} \\
&= \Pi_1(0) + (\theta\lambda_1 + (1-\theta)\lambda_2) \begin{bmatrix} \dfrac{\mathscr{S}(X)}{2} & -X + X_1 \\ * & -\mathscr{S}(X_1) + \dfrac{\mathscr{S}(X)}{2} \end{bmatrix} \\
&= \theta\Pi_1(\lambda_1) + (1-\theta)\Pi_1(\lambda_2) > 0.
\end{aligned}$$

By applying the Schur complement to $\Pi_2(\tilde{h}_k)$ as proposed in (21), we have

$$\Pi_2(\tilde{h}_k) = \Sigma(\tilde{h}_k) + \Xi = \Sigma(0) + \tilde{h}_k\Delta + \Xi < 0,$$

where $\Delta = [\Delta_{ij}]_{9n \times 9n}$ denotes a symmetric matrix, $\Delta_{11} = S + \frac{\delta\lambda_2}{2}S + \delta\mathscr{S}(X)$, $\Delta_{12} = \frac{\lambda_2}{4}S + \frac{1}{2}\mathscr{S}(X)$, $\Delta_{14} = -2\delta(X - X_1)$, $\Delta_{22} = U$, $\Delta_{24} = -X + X_1$, $\Delta_{44} = \delta\mathscr{S}(X) - 2\delta\mathscr{S}(X_1)$, other blocks are zero matrices. Thus, we obtain

$$\begin{aligned}
\Pi_2(h_k) &= \Sigma(0) + h_k\Delta + \Xi \\
&= \Sigma(0) + (\theta\lambda_1 + (1-\theta)\lambda_2)\Delta + \Xi \\
&= \theta\Pi_2(\lambda_1) + (1-\theta)\Pi_2(\lambda_2) < 0.
\end{aligned}$$

Similarly, $\Pi_3(\tilde{h}_k) < 0$ can guarantee that $\Pi_3(h_k) < 0$. Furthermore, the inequality $\Pi_4 < 0$ is always true because it is independent of the parameter h_k. Thus, the proof is completed.

Remark 4. Considering the intermittent sensor breakdowns and limited network resources, aperiodic sampling technique may be more practical and meaningful in contrast with the periodic sampling technique. However, the existence of h_k can result in the nonlinearity and increase the complexity of (9)–(12) as shown in Theorem 1. It can be seen from the proof of Theorem 2 that (9)–(12) are convex in $[\lambda_1, \lambda_2]$. This implies that if they are feasible for λ_1 and λ_2, then they are feasible for all $h_k \in [\lambda_1, \lambda_2]$. In other words, Theorem 2 establishes an LMI-based criterion, in which h_k is only restricted at the two endpoints λ_1 and λ_2. This criterion contains four LMIs and $(11n^2 + 5n)$ scalar decision variables and can be tested easily using the LMI toolbox in MATLAB.

Remark 5. It is obvious that Theorem 2 is the necessary condition of Theorem 1. To prove that Theorem 2 is the sufficient condition of Theorem 1, Schur complement and matrix decomposition can be used so that $\Pi_i(h_k)$ can be expressed as a linear combination of $\Pi_i(\lambda_1)$ and $\Pi_i(\lambda_2)$. To be specific, $\Pi_i(h_k) = \theta\Pi_i(\lambda_1) + (1-\theta)\Pi_i(\lambda_2)$ for $0 \leqslant \theta \leqslant 1$, $i = 1, 2, 3$. It is obvious that the sign of $\Pi_i(h_k)$ is determined using the sign of $\Pi_i(\lambda_1)$ and $\Pi_i(\lambda_2)$. Hence, the sufficiency of the theorem can be proved.

It is noteworthy that LMIs (21) are nonlinear with respect to the feedback gain F. Hence, it is necessary to provide a design method for F. Next, it is clear that F can be designed by solving a group of LMIs.

Theorem 3. For given scalars $\alpha \geqslant 0$, $\beta > 0$, $\gamma \geqslant 0$, $\delta > 0$, $\lambda_2 \geqslant \lambda_1 > 0$, $\rho_1 > 0$, $\rho_2 > 0$, and $\rho_3 > 0$, system (1) can be globally asymptotically stabilized using the controller (5), if there exist matrices $P > 0$, $Q > 0$, $R > 0$, $S > 0$, $U > 0$, $\Omega \geqslant 0$, diagonal matrices $N_1 > 0$, $N_2 > 0$, $Z_1 > 0$, $Z_2 > 0$, $Z_3 > 0$, $Z_4 > 0$, and arbitrary matrices Y_1, Y_2, X, X_1, W, V, for any $\tilde{h}_k \in \{\lambda_1, \lambda_2\}$, such that

$$\begin{bmatrix} P + \tilde{h}_k \dfrac{\mathscr{S}(X)}{2} & \tilde{h}_k(-X + X_1) \\ * & \tilde{h}_k\left(-\mathscr{S}(X_1) + \dfrac{\mathscr{S}(X)}{2}\right) \end{bmatrix} > 0, \tag{22}$$

$$\begin{bmatrix} \widetilde{\Sigma}(\tilde{h}_k) & \xi_1 & \xi_2 & \xi_3 & \xi_4 & \Phi_1 + \rho_1\Upsilon_1 \\ * & -Z_1 & 0 & 0 & 0 & 0 \\ * & * & -Z_2 & 0 & 0 & 0 \\ * & * & * & -Z_3 & 0 & 0 \\ * & * & * & * & -Z_4 & 0 \\ * & * & * & * & * & -\rho_1 W - \rho_1 W^{\mathrm{T}} \end{bmatrix} < 0, \tag{23}$$

$$\begin{bmatrix} \widetilde{\Theta}(\tilde{h}_k) & \xi_1 & \xi_2 & \xi_3 & \xi_4 & \Phi_1 + \rho_2\Upsilon_1 \\ * & -Z_1 & 0 & 0 & 0 & 0 \\ * & * & -Z_2 & 0 & 0 & 0 \\ * & * & * & -Z_3 & 0 & 0 \\ * & * & * & * & -Z_4 & 0 \\ * & * & * & * & * & -\rho_2 W - \rho_2 W^{\mathrm{T}} \end{bmatrix} < 0, \tag{24}$$

$$\begin{bmatrix} \widetilde{\Gamma} & \eta_1 & \eta_2 & \eta_3 & \eta_4 & \Phi_2 + \rho_3\Upsilon_2 \\ * & -Z_1 & 0 & 0 & 0 & 0 \\ * & * & -Z_2 & 0 & 0 & 0 \\ * & * & * & -Z_3 & 0 & 0 \\ * & * & * & * & -Z_4 & 0 \\ * & * & * & * & * & -\rho_3 W - \rho_3 W^{\mathrm{T}} \end{bmatrix} < 0, \tag{25}$$

where $\rho_1 > 0$, $\rho_2 > 0$, and $\rho_3 > 0$ represent the tuning parameters, $\widetilde{\Sigma}(\tilde{h}_k) = [\widetilde{\Sigma}_{ij}]_{9n\times 9n}$, $\widetilde{\Theta}(\tilde{h}_k) = [\widetilde{\Theta}_{ij}]_{9n\times 9n}$, $\widetilde{\Gamma} = [\widetilde{\Gamma}_{ij}]_{8n\times 8n}$, $\widetilde{\Sigma}_{14} = -\frac{2U}{\lambda_2}\mathrm{e}^{-2\delta\lambda_2} - V + (2\delta\tilde{h}_k - 1)(-X + X_1)$, $\widetilde{\Sigma}_{24} = \tilde{h}_k(-X + X_1) - V$, $\widetilde{\Theta}_{14} = -\frac{2U}{\lambda_2}\mathrm{e}^{-2\delta\lambda_2} - V + X - X_1$, $\widetilde{\Theta}_{24} = -V$, $\widetilde{\Gamma}_{14} = \Omega - V$, $\widetilde{\Gamma}_{24} = -V$, and the remaining terms of the matrices $\widetilde{\Sigma}(\tilde{h}_k)$, $\widetilde{\Theta}(\tilde{h}_k)$, $\widetilde{\Gamma}$ are the same as the corresponding elements in matrices $\Sigma(\tilde{h}_k)$, $\Theta(\tilde{h}_k)$, $\Gamma(\tilde{h}_k)$ defined in Theorem 2, respectively. And, $\Phi_1 = \mathrm{col}\{-Y_1^{\mathrm{T}} + W, -Y_2^{\mathrm{T}} + W, 0_{7n\times n}\}$, $\Phi_2 = \mathrm{col}\{-Y_1^{\mathrm{T}} + W, -Y_2^{\mathrm{T}} + W, 0_{6n\times n}\}$, $\Upsilon_1 = \mathrm{col}\{0_{3n\times n}, V^{\mathrm{T}}, 0_{5n\times n}\}$, $\Upsilon_2 = \mathrm{col}\{0_{3n\times n}, V^{\mathrm{T}}, 0_{4n\times n}\}$. Furthermore, the feedback gain can be expressed as $F = W^{-1}V$.

Proof. Applying Lemma 2 to (23), we obtain

$$\begin{bmatrix} \widetilde{\Sigma}(\tilde{h}_k) & \xi_1 & \xi_2 & \xi_3 & \xi_4 \\ * & -Z_1 & 0 & 0 & 0 \\ * & * & -Z_2 & 0 & 0 \\ * & * & * & -Z_3 & 0 \\ * & * & * & * & -Z_4 \end{bmatrix} + \mathscr{S}\left(\begin{bmatrix} \Phi_1 \\ 0 \\ 0 \\ 0 \\ 0 \end{bmatrix} W^{-1} \begin{bmatrix} \Upsilon_1^{\mathrm{T}} & 0 & 0 & 0 & 0 \end{bmatrix}\right) < 0,$$

which is equivalent to

$$\begin{bmatrix} \widetilde{\Sigma}(\tilde{h}_k) + \mathscr{S}(\Phi_1 W^{-1}\Upsilon_1^{\mathrm{T}}) & \xi_1 & \xi_2 & \xi_3 & \xi_4 \\ * & -Z_1 & 0 & 0 & 0 \\ * & * & -Z_2 & 0 & 0 \\ * & * & * & -Z_3 & 0 \\ * & * & * & * & -Z_4 \end{bmatrix} < 0.$$

According to the expressions of $\widetilde{\Sigma}(\tilde{h}_k)$, Φ_1 and Υ_1, the above inequality is equivalent to

$$\begin{bmatrix} \Sigma(\tilde{h}_k) & \xi_1 & \xi_2 & \xi_3 & \xi_4 \\ * & -Z_1 & 0 & 0 & 0 \\ * & * & -Z_2 & 0 & 0 \\ * & * & * & -Z_3 & 0 \\ * & * & * & * & -Z_4 \end{bmatrix} < 0.$$

Furthermore, $\Pi_2(\tilde{h}_k) < 0$ can be derived from (23). $\Pi_3(\tilde{h}_k) < 0$ and $\Pi_4 < 0$ can be derived from (24) and (25) in the same manner, respectively. Thus, the proof is completed.

4 Numerical simulations

Consider DMNNs (1) with $n = 2$, $f_j(x_j) = \tanh(x_j)$, $j = 1, 2$, $\tau(t) = \frac{\mathrm{e}^t}{1+\mathrm{e}^t} \leqslant 1$, $d_1 = d_2 = 1$, and

$$a_{11}(x_1(t)) = \begin{cases} 1, & |x_1(t)| \leqslant 1.3, \\ 1.2, & |x_1(t)| > 1.3, \end{cases} \qquad a_{12}(x_2(t)) = \begin{cases} -3.7, & |x_2(t)| \leqslant 1.3, \\ -2.2, & |x_2(t)| > 1.3, \end{cases}$$

$$a_{21}(x_1(t)) = \begin{cases} -0.1, & |x_1(t)| \leqslant 1.3, \\ -0.12, & |x_1(t)| > 1.3, \end{cases} \qquad a_{22}(x_2(t)) = \begin{cases} 2.8, & |x_2(t)| \leqslant 1.3, \\ 3.3, & |x_2(t)| > 1.3, \end{cases}$$

$$b_{11}(x_1(t)) = \begin{cases} -3.7, & |x_1(t)| \leqslant 1.3, \\ -4.5, & |x_1(t)| > 1.3, \end{cases} \qquad b_{12}(x_2(t)) = \begin{cases} -0.5, & |x_2(t)| \leqslant 1.3, \\ -0.1, & |x_2(t)| > 1.3, \end{cases}$$

$$b_{21}(x_1(t)) = \begin{cases} -1.08, & |x_1(t)| \leqslant 1.3, \\ -2.12, & |x_1(t)| > 1.3, \end{cases} \qquad b_{22}(x_2(t)) = \begin{cases} -2.5, & |x_2(t)| \leqslant 1.3, \\ -2.36, & |x_2(t)| > 1.3. \end{cases}$$

Figure 1 shows the chaotic attractor of DMNNs (1) with the initial conditions $(-1.3, 0.8)^{\mathrm{T}}$ and the above system parameters. From Figure 1, it is clear that the system (1) without controller is unstable.

By calculation, we obtain

$$\begin{aligned} &\tau = 1, \quad \mu = 0.25, \quad M_1 = \mathrm{diag}\{0, 0\}, \quad M_2 = \mathrm{diag}\{0.5, 0.5\}, \\ &A = \begin{bmatrix} 1.1 & -2.95 \\ -0.11 & 3.05 \end{bmatrix}, \quad B = \begin{bmatrix} -4.1 & -0.3 \\ -1.6 & -2.43 \end{bmatrix}, \quad D = \begin{bmatrix} 1 & 0 \\ 0 & 1 \end{bmatrix}, \\ &A_1 = \begin{bmatrix} \sqrt{0.1} & \sqrt{0.75} & 0 & 0 \\ 0 & 0 & \sqrt{0.01} & \sqrt{0.25} \end{bmatrix}, \quad B_1 = \begin{bmatrix} \sqrt{0.4} & \sqrt{0.2} & 0 & 0 \\ 0 & 0 & \sqrt{0.52} & \sqrt{0.07} \end{bmatrix}, \\ &A_2^{\mathrm{T}} = \begin{bmatrix} \sqrt{0.1} & 0 & \sqrt{0.01} & 0 \\ 0 & \sqrt{0.75} & 0 & \sqrt{0.25} \end{bmatrix}, \quad B_2^{\mathrm{T}} = \begin{bmatrix} \sqrt{0.4} & 0 & \sqrt{0.52} & 0 \\ 0 & \sqrt{0.2} & 0 & \sqrt{0.07} \end{bmatrix}. \end{aligned}$$

Herein, we present some comparisons to illustrate the advantages of RSETC (4) over the existing triggering mechanisms. We compare Theorems 2 and 3 with the existing results obtained based on SETC [33–35].

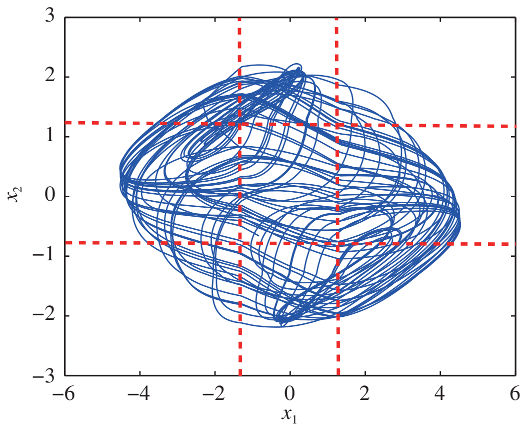

Figure 1 (Color online) The chaotic attractor of system (1) with initial conditions $(-1.3, 0.8)^{\mathrm{T}}$.

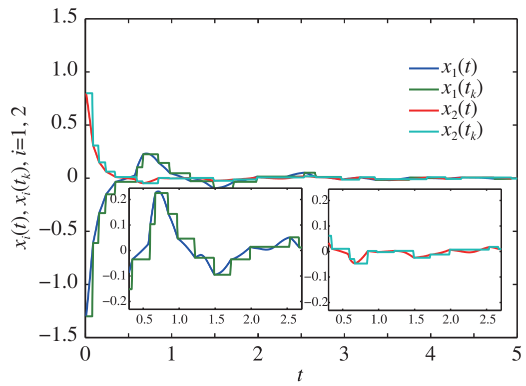

Figure 2 (Color online) State trajectories of $x_i(t)$ and the sampled data $x_i(t_k)$ $(i = 1, 2)$.

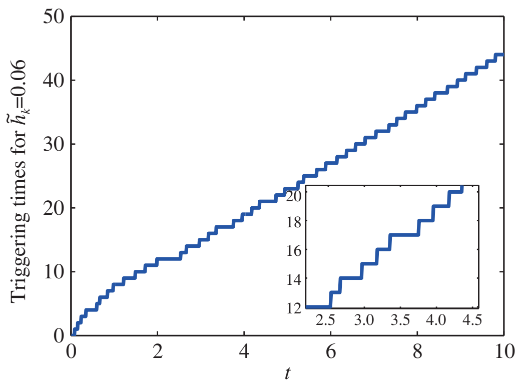

Figure 3 (Color online) Triggering times.

Comparison based on Theorem 2. Let $\gamma = 0.01$, $\delta = 0.1$, $\lambda_1 = 0.01$, $\lambda_2 = 0.06$, and the feedback gain $F = \begin{bmatrix} 8 & 0.2 \\ 0.1 & 9 \end{bmatrix}$. When $\tilde{h}_k = 0.01$, the trigger matrix can be solved as $\Omega = \begin{bmatrix} 2.8662 & -0.0730 \\ -0.0730 & 2.9409 \end{bmatrix}$ based on Theorem 2. Similarly, for $\tilde{h}_k = 0.06$, the trigger matrix can be solved as $\Omega = \begin{bmatrix} 6.1214 & -0.6842 \\ -0.6842 & 7.2381 \end{bmatrix}$. In the simulations, the simulation time is set as $T_{\text{time}} = 10$ s. t_s and m_s represent the triggering times and data transmission rate, respectively. Figure 2 shows the time response of the closed-loop system (6) with $\tilde{h}_k = 0.06$. According to Theorem 2, system (1) achieves global stabilization under controller (5) using the RSETC scheme (4). Figure 3 shows the triggering times when using RSETC (4) with $\tilde{h}_k = 0.06$. Figures 4 and 5 show the triggering instants and the corresponding triggering intervals based on the SETC and RSETC schemes (4), respectively. Obviously, the average triggering interval of RSETC is much larger than that of SETC, which indicates that RSETC can significantly reduce the amount of triggering times.

From the comparison data in Table 1, it is obvious that the amount of triggering times of RSETC has decreased by more than 66% compared with SETC. Furthermore, the simulation results presented in Tables 1 and 2 show that the amount of triggering times relates to the trigger parameters α and β. Intuitively, a larger α and a smaller β can result in a smaller triggering times.

Comparison based on Theorem 3. Let $\gamma = 0.001$, $\delta = 0.1$, $\lambda_1 = 0.01$, $\lambda_2 = 0.014$. When $\tilde{h}_k = 0.01$, by solving LMIs (22)–(25), we can obtain the feedback gain $F = \begin{bmatrix} 36.7909 & 3.7137 \\ 3.7521 & 30.3402 \end{bmatrix}$, and the trigger matrix $\Omega = \begin{bmatrix} 0.0530 & 0.0009 \\ 0.0009 & 0.0562 \end{bmatrix}$. Similarly, for $\tilde{h}_k = 0.014$, the feedback gain can be calculated as $F = \begin{bmatrix} 35.1410 & 1.1940 \\ 1.5200 & 32.0547 \end{bmatrix}$, and the trigger matrix can be solved as $\Omega = \begin{bmatrix} 0.5759 & -0.0325 \\ -0.0325 & 0.6141 \end{bmatrix}$. Figure 6 illustrates the time response of the closed-loop system (6) with $\tilde{h}_k = 0.014$. According to Theorem 3, system (1) achieves global stabilization

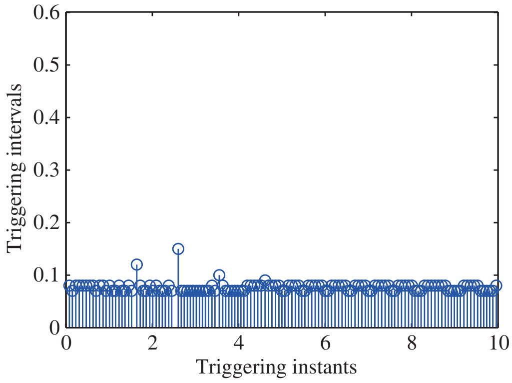

Figure 4 (Color online) Triggering instants and triggering intervals based on the SETC scheme.

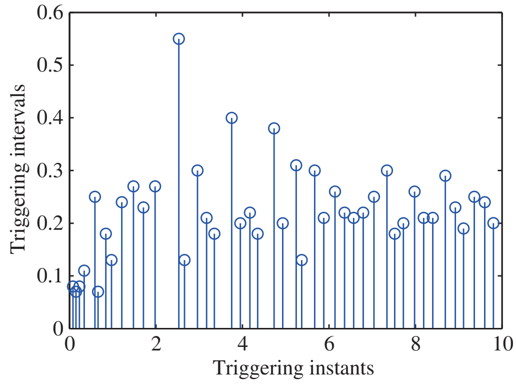

Figure 5 (Color online) Triggering instants and triggering intervals based on the RSETC scheme.

Table 1 Comparison of triggering times t_s for RSETC and SETC schemes at $\tilde{h}_k = 0.06$

Method	Parameters	t_s	m_s (%)
SETC [33–35]	$\alpha = 0,\ \beta = 1$	130	100
RSETC	$\alpha = 0.01,\ \beta = 1$	55	42
RSETC	$\alpha = 0.1,\ \beta = 1$	44	33

Table 2 Comparison of triggering times t_s for different β at $\tilde{h}_k = 0.06$

Method	Parameters	t_s	m_s (%)
RSETC	$\alpha = 0.1,\ \beta = 5$	127	100
RSETC	$\alpha = 0.1,\ \beta = 2$	93	73
RSETC	$\alpha = 0.1,\ \beta = 1$	44	34

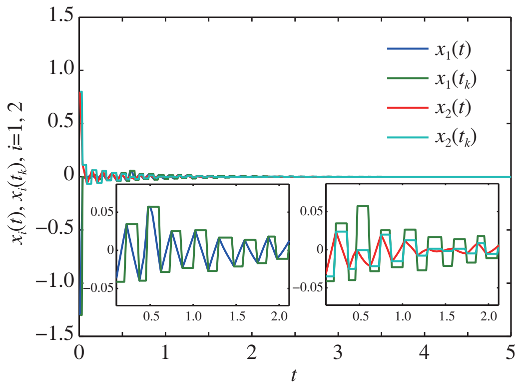

Figure 6 (Color online) State trajectories of $x_i(t)$ and the sampled data $x_i(t_k)$ $(i = 1, 2)$.

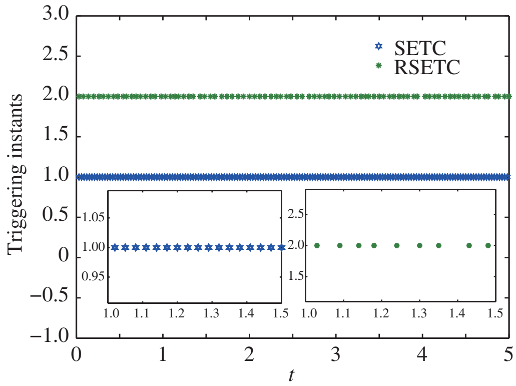

Figure 7 (Color online) Triggering instants under the RSETC (4) and SETC schemes.

Table 3 Comparison of the triggering times t_s between RSETC and SETC schemes at $\tilde{h}_k = 0.014$

Method	Parameters	t_s	m_s (%)
SETC [33–35]	$\alpha = 0, \beta = 5$	333	100
RSETC	$\alpha = 0.001,\ \beta = 5$	235	70
RSETC	$\alpha = 0.01,\ \beta = 5$	227	68

using the RSETC scheme (4). Figure 7 shows the event-triggering instants when using RSETC (4) and SETC schemes. In Figure 7, the values “2” and “1” denote the triggering instants for RSETC (4) and SETC, respectively.

From Table 3, it is obvious that the amount of the triggering times for the RSETC scheme has fallen

Table 4 Comparison of triggering times t_s for different β at $\tilde{h}_k = 0.014$

Method	Parameters	t_s	m_s (%)
RSETC	$\alpha = 0.01$, $\beta = 7$	290	100
RSETC	$\alpha = 0.01$, $\beta = 5$	227	78
RSETC	$\alpha = 0.01$, $\beta = 3$	170	58

by more than 31% compared with the SETC scheme. This suggests that the network resources can be significantly saved by introducing an exponential decay term $\alpha e^{-\beta t}$ and meanwhile, the performance of the closed-loop system can be preserved. Table 4 shows that a smaller value of β in the RSETC scheme corresponds to a smaller triggering times when the parameter α remains unchanged.

5 Conclusion

In this paper, we explored global stabilization of DMNNs within the framework of event-triggered control. We developed a RSETC scheme by replacing constant sampling with variable sampling and incorporating an exponential decay term into the predefined threshold function. We showed that introducing the exponential decay term can increase the threshold function moderately and can help to reduce the amount of triggering times effectively. We also constructed a time-dependent and piecewise-defined Lyapunov functional $V(t)$, which considers the available information of system states over each interval $[t_k, t_k + h_k)$ and $[t_k + h_k, t_{k+1})$. Subsequently, we established two less-conservative criteria (i.e., Theorems 1 and 2) to guarantee the globally asymptotical stability of closed-loop DMNNs. We also proposed a method for the co-design of both the feedback gain and the trigger matrix by employing a decoupling approach, as shown in Theorem 3. Finally, we demonstrated the feasibility and superiority of the proposed event-trigger scheme and the theoretical results by a numerical simulation example. Our future work would focus on the actuator saturation and packet dropouts problems of the DMNNs.

Acknowledgements This work was supported by National Natural Science Foundation of China (Grant Nos. 61973199, 61473178, 61573008). We would thank anonymous reviewers for their valuable suggestions.

References

1 Chua L. Memristor-the missing circuit element. IEEE Trans Circ Theory, 1971, 18: 507–519

2 Wang L M, Shen Y. Design of controller on synchronization of memristor-based neural networks with time-varying delays. Neurocomputing, 2015, 147: 372–379

3 Yang X S, Ho D W C. Synchronization of delayed memristive neural networks: robust analysis approach. IEEE Trans Cybern, 2016, 46: 3377–3387

4 Yang X S, Cao J D, Liang J L. Exponential synchronization of memristive neural networks with delays: interval matrix method. IEEE Trans Neural Netw Learn Syst, 2017, 28: 1878–1888

5 Fan Y J, Huang X, Li Y X, et al. Aperiodically intermittent control for quasi-synchronization of delayed memristive neural networks: an interval matrix and matrix measure combined method. IEEE Trans Syst Man Cybern Syst, 2019, 49: 2254–2265

6 Li N, Cao J D. Lag synchronization of memristor-based coupled neural networks via ω-measure. IEEE Trans Neural Netw Learn Syst, 2016, 27: 686–697

7 Liu H J, Wang Z D, Shen B, et al. Event-triggered H_∞ state estimation for delayed stochastic memristive neural networks with missing measurements: the discrete time case. IEEE Trans Neural Netw Learn Syst, 2018, 29: 3726–3737

8 Cao J D, Li R X. Fixed-time synchronization of delayed memristor-based recurrent neural networks. Sci China Inf Sci, 2017, 60: 032201

9 Jia J, Huang X, Li Y X, et al. Global stabilization of fractional-order memristor-based neural networks with time delay. 2019. doi: 10.1109/TNNLS.2019.2915353

10 Choi H, Jung H, Lee J, et al. An electrically modifiable synapse array of resistive switching memory. Nanotechnology, 2009, 20: 345201

11 Kim H, Sah M P, Yang C J, et al. Neural synaptic weighting with a pulse-based memristor circuit. IEEE Trans Circ Syst I, 2012, 59: 148–158

12 Liao X F, Yu J B. Robust stability for interval Hopfield neural networks with time delay. IEEE Trans Neural Netw, 1998, 9: 1042–1045

13 Wu A L, Zeng Z G. Exponential stabilization of memristive neural networks with time delays. IEEE Trans Neural Netw Learn Syst, 2012, 23: 1919–1929

14 Guo Z Y, Wang J, Yan Z. Global exponential dissipativity and stabilization of memristor-based recurrent neural networks with time-varying delays. Neural Netw, 2013, 48: 158–172
15 Zhang G D, Shen Y. Exponential stabilization of memristor-based chaotic neural networks with time-varying delays via intermittent control. IEEE Trans Neural Netw Learn Syst, 2015, 26: 1431–1441
16 Wen S P, Huang T W, Zeng Z G, et al. Circuit design and exponential stabilization of memristive neural networks. Neural Netw, 2015, 63: 48–56
17 Ding S B, Wang Z S, Rong N N, et al. Exponential stabilization of memristive neural networks via saturating sampled-data control. IEEE Trans Cybern, 2017, 47: 3027–3039
18 Zhang W, Branicky M S, Phillips S M. Stability of networked control systems. IEEE Control Syst, 2001, 21: 84–99
19 Ge X H, Yang F W, Han Q L. Distributed networked control systems: a brief overview. Inf Sci, 2017, 380: 117–131
20 Hespanha J P, Naghshtabrizi P, Xu Y G. A survey of recent results in networked control systems. Proc IEEE, 2007, 95: 138–162
21 Ogren P, Fiorelli E, Leonard N E. Cooperative control of mobile sensor networks: adaptive gradient climbing in a distributed environment. IEEE Trans Autom Control, 2004, 49: 1292–1302
22 Walsh G C, Ye H. Scheduling of networked control systems. IEEE Control Syst, 2001, 21: 57–65
23 Tabuada P. Event-triggered real-time scheduling of stabilizing control tasks. IEEE Trans Autom Control, 2007, 52: 1680–1685
24 Borgers D P, Heemels W P M H. Event-separation properties of event-triggered control systems. IEEE Trans Autom Control, 2014, 59: 2644–2656
25 Heemels W P M H, Donkers M C F, Teel A R. Periodic event-triggered control for linear systems. IEEE Trans Autom Control, 2013, 58: 847–861
26 Zhang X M, Han Q L, Zhang B L. An overview and deep investigation on sampled-data-based event-triggered control and filtering for networked systems. IEEE Trans Ind Inf, 2017, 13: 4–16
27 Lunze J, Lehmann D. A state-feedback approach to event-based control. Automatica, 2010, 46: 211–215
28 Yue D, Tian E G, Han Q L. A delay system method for designing event-triggered controllers of networked control systems. IEEE Trans Autom Control, 2013, 58: 475–481
29 Wen S P, Zeng Z G, Chen M Z, et al. Synchronization of switched neural networks with communication delays via the event-triggered control. IEEE Trans Neural Netw Learn Syst, 2017, 28: 2334–2343
30 Wang J, Chen M S, Shen H. Event-triggered dissipative filtering for networked semi-Markov jump systems and its applications in a mass-spring system model. Nonlinear Dyn, 2017, 87: 2741–2753
31 Shen B, Wang Z D, Qiao H. Event-triggered state estimation for discrete-time multidelayed neural networks with stochastic parameters and incomplete measurements. IEEE Trans Neural Netw Learn Syst, 2017, 28: 1152–1163
32 Duan G P, Xiao F, Wang L. Hybrid event- and time-triggered control for double-integrator heterogeneous networks. Sci China Inf Sci, 2019, 62: 022203
33 Selivanov A, Fridman E. A switching approach to event-triggered control. In: Proceedings of the 54th IEEE Conference on Decision and Control, Osaka, 2015. 5468–5473
34 Selivanov A, Fridman E. Event-triggered H_∞ control: a switching approach. IEEE Trans Autom Control, 2016, 61: 3221–3226
35 Fei Z Y, Guan C X, Gao H J. Exponential synchronization of networked chaotic delayed neural network by a hybrid event trigger scheme. IEEE Trans Neural Netw Learn Syst, 2018, 29: 2558–2567
36 Fan Y J, Huang X, Shen H, et al. Switching event-triggered control for global stabilization of delayed memristive neural networks: an exponential attenuation scheme. Neural Netw, 2019, 117: 216–224
37 Filippov A F. Differential Equations with Discontinuous Righthand Sides. Boston: Kluwer, 1988
38 Aubin J P, Cellina A. Differential Inclusions. Berlin: Springer, 1984
39 Fridman E. A refined input delay approach to sampled-data control. Automatica, 2010, 46: 421–427
40 Suh Y S. Stability and stabilization of nonuniform sampling systems. Automatica, 2008, 44: 3222–3226
41 Seuret A, Gouaisbaut F. Wirtinger-based integral inequality: application to time-delay systems. Automatica, 2013, 49: 2860–2866
42 Zhou J P, Park J H, Ma Q. Non-fragile observer-based H_∞ control for stochastic time-delay systems. Appl Math Comput, 2016, 291: 69–83
43 Boyd S, El Ghaoui L, Feron E, et al. Linear Matrix Inequalities in System and Control Theory. Philadelphia: SIAM, 1994